

Neuronal Pentraxin I Promotes Hypoxic-Ischemic Neuronal Injury by Impairing Mitochondrial Biogenesis via Interactions With Active Bax[6A7] and Mitochondrial Hexokinase II

ASN Neuro
Volume 13: 1–16
© The Author(s) 2021
Article reuse guidelines:
sagepub.com/journals-permissions
DOI: 10.1177/17590914211012888
journals.sagepub.com/home/asn


Md Al Rahim^{1,2,3} , Shabarish Thatipamula^{1,2},
Giulio M. Pasinetti^{3,4}, and Mir Ahamed Hossain^{1,2}

Abstract

Mitochondrial dysfunction is a key mechanism of cell death in hypoxic-ischemic brain injury. Neuronal pentraxin I (NPI) has been shown to play crucial roles in mitochondria-mediated neuronal death. However, the underlying mechanism(s) of NPI-induced mitochondrial dysfunction in hypoxia-ischemia (HI) remains obscure. Here, we report that NPI induction following HI and its subsequent localization to mitochondria, leads to disruption of key regulatory proteins for mitochondrial biogenesis. Brain mitochondrial DNA (mtDNA) content and mtDNA-encoded subunit I of complex IV (mtCOX-I) expression was increased post-HI, but not the nuclear DNA-encoded subunit of complex II (nSDH-A). Up-regulation of mitochondrial proteins COXIV and HSP60 further supported enhanced mtDNA function. NPI interaction with active Bax (Bax6A7) was increased in the brain after HI and in oxygen-glucose deprivation (OGD)-induced neuronal cultures. Importantly, NPI colocalized with mitochondrial hexokinase II (mtHKII) following OGD leading to HKII dissociation from mitochondria. Knockdown of NPI or SB216763, a GSK-3 inhibitor, prevented OGD-induced mtHKII dissociation and cellular ATP decrease. NPI also modulated the expression of mitochondrial transcription factor A (*Tfam*) and peroxisome proliferator-activated receptor γ coactivator-1 α (PGC-1 α), regulators of mitochondrial biogenesis, following HI. Together, we reveal crucial roles of NPI in mitochondrial biogenesis involving interactions with Bax[6A7] and mtHKII in HI brain injury.

Keywords

hypoxia-ischemia, neonatal brain injury, neuronal pentraxin I, hexokinase II, mitochondrial transcription factor A, peroxisome proliferator-activated receptor γ coactivator-1 α

Received January 9, 2021; Revised February 22, 2021; Accepted for publication March 8, 2021

Mitochondria play essential roles in the maintenance of the viability of neurons or degeneration of neurons in response to brain injury (Halestrap et al., 2000; Achanta et al., 2005; Mattson et al., 2008). Mitochondrial failure is a key to the pathobiology of ischemic brain injury where cellular bioenergetics failure results in a severe injury to the brain (Blomgren and Hagberg, 2006; Yin et al., 2008). However, how changes in specific mitochondrial properties relate to neuronal injury/degeneration is not completely understood.

¹Hugo W. Moser Research Institute at Kennedy Krieger, Baltimore, Maryland, United States

²Department of Neurology, Johns Hopkins University School of Medicine, Baltimore, Maryland, United States

³Department of Neurology, Icahn School of Medicine at Mount Sinai, New York, New York, United States

⁴James J. Peters Veterans Affairs Medical Center, Bronx, New York, United States

Corresponding Author:

Md Al Rahim, Department of Neurology, Icahn School of Medicine at Mount Sinai, 1468 Madison Avenue, New York, NY 10029, United States.

Email: mdal.rahim@mssm.edu



In previous studies, we have shown the involvement of neuronal pentraxin 1 (NP1) in mitochondria-mediated hypoxic-ischemic (HI) neuronal injury (Al Rahim et al., 2013). Mitochondrial biogenesis is regulated through the coordinated actions of both nuclear and mitochondrial genomes to ensure that the organelles are replenished on a regular basis. Although the involvement of mitochondria in neuronal injury has been well studied, much less is known about the role of mitochondrial biogenesis after cerebral HI (Yin et al., 2008), and the involvement of NP1 into this mechanism in response to hypoxia-ischemia (HI) is essentially unknown.

The mechanisms of brain injury following HI are multifarious, which encompass energy depletion, excitotoxicity, oxidative stress, generation of reactive oxygen species (ROS) and apoptosis (Barks and Silverstein, 1992; Cheng et al., 1998; Halestrap et al., 2000; Achanta et al., 2005). In the intrinsic pathway of apoptosis, Bax translocate to mitochondria and forms a large homo-oligomer complex that permeabilizes the outer mitochondrial membrane (OMM), allowing the release of pro-apoptotic factors, including cytochrome *c* (Cyt C) (Youle and Strasser, 2008). We have previously shown that NP1 facilitates translocation of Bax to mitochondria in OGD-exposed hippocampal neurons (Al Rahim et al., 2013). On the other hand, mitochondria bound hexokinase (HK) type II (HKII) plays an important role in maintaining the integrity of the OMM and neuronal survival, and its detachment from mitochondria triggers apoptosis (Chiara et al., 2008; Gall et al., 2011). It has been shown that the pro-survival kinase Akt (Majewski et al., 2004) promotes HKII binding to the voltage-dependent anion channel (VDAC; Pastorino and Hoek, 2003; Vyssokikh and Brdiczka, 2004), a protein that favors movement of small molecules across the OMM (Colombini, 2004). Dissociation of HKII transmits a potent death signal (Zaid et al., 2005) that is elicited when GSK-3 β , a downstream kinase inhibited by Akt, phosphorylates HK docking site on VDAC (Pastorino et al., 2005). Mitochondrial HKII (mtHKII) interferes with Bax binding to mitochondria and, Cyt C release; in addition, HKII overexpression inhibits Bax-induced mitochondrial dysfunction and cell death (Pastorino et al., 2002). Considering our findings on the involvement of NP1 in facilitating Bax translocation to mitochondria (Al Rahim et al., 2013), GSK-3 α/β -dependent NP1 induction (Russell et al., 2011) and the reported cross-talk between Bax and HKII in mitochondria (Pastorino et al., 2002), we hypothesize that NP1 interacts with active Bax and facilitates translocation to mitochondria, and the NP1-Bax[6A7] in turn promote dissociation of HKII from the docking site on the VDAC in mitochondria resulting in neuronal injury/death following HI.

Ischemic damage to mitochondria includes ROS generation, mitochondrial DNA (mtDNA) damage, and impairment of oxidative phosphorylation (Hagberg, 2004; Galluzzi et al., 2009). In addition, mitochondria also induce endogenous protective signals, e.g. stimulation of mitochondrial biogenesis to compensate for the deleterious effects of hypoxic-ischemic damage to the brain (Fiskum, 2000; Hagberg, 2004; St-Pierre et al., 2006). Whereas, under prolonged hypoxic-ischemic stress, mitochondrial renewal mechanisms fail (Chen et al., 2001). The peroxisome proliferator-activated receptor γ coactivator-1 α (PGC-1 α) is a co-transcriptional regulation factor that induces mitochondrial biogenesis by activating different transcription factors, including nuclear respiratory factors 1 and 2 proteins (NRF-1 and NRF-2) and the mitochondrial transcription factor A (TFAM; Wu et al., 2001; Scarpulla, 2006). The NRF-1 and NRF-2 mediate expression of multiple nuclear genes encoding for mitochondrial proteins, while TFAM is involved in mtDNA maintenance and drives the transcription and replication of mtDNA (Scarpulla, 2006). Recent reports suggested enhanced mitochondrial biogenesis immediate after hypoxic-ischemic brain injury in a rat model (Yin et al., 2008; Valerio et al., 2011). However, to our knowledge, no study has reported yet the effects on mitochondrial biogenesis during the delayed neuronal death and the effects of NP1 induction on transcriptional regulation of mitochondrial biogenesis.

In the present study, we have investigated the contribution of NP1 to the biochemical cascades of mitochondria-mediated cell death evoked by HI and effects on mitochondrial protein expression and bioenergetics in the hypoxic-ischemic brain injury. Here, we report that NP1 is preferentially translocated to mitochondria following HI, and that NP1 interacts with the pro-death Bax and impairs mtHKII function in the mitochondria to induce cell death. In addition, we show for the first time that persistent induction of NP1 following HI impairs mitochondrial biogenic programs, whereas, deletion of NP1 gene displayed enhanced mitochondrial biogenesis as evident by increased expression of PGC-1 α and TFAM leading to neuroprotection against hypoxic-ischemic brain injury.

Materials and Methods

Unilateral Cerebral Hypoxia-Ischemia

All procedures involving animals were performed in accordance with the NIH guide for the Care and Use of Laboratory Animals and were approved by The Johns Hopkins University Animal Care and Use Committee. Common carotid artery (CCA) occlusion combined with controlled hypoxia in postnatal day

8 wild type (WT) and NP1 knockout (NP1-KO) mouse pups was performed as described previously (Hossain et al., 2004; Al Rahim et al., 2013), to produce hypoxic-ischemic brain injury. Briefly, under deep inhalant anesthesia (isoflurane in an oxygen-nitrous oxide mixture delivered via a Drager vaporizer), a 3–4 mm incision was made in the neck, and the right common carotid artery was isolated, double ligated, and cut between the ligatures. After the surgical procedure, the animals recovered for 2 h in a temperature-controlled incubator, and then animals were placed in an enclosed, vented 500 ml Plexiglas chamber that was partially submerged in 36°C water. Hypoxia was induced by continuous flow of warm, humidified gas (10% oxygen, balanced nitrogen) for 1 h. A subset of control animals were mock-treated with a small incision in their neck without CCA occlusion and placed in the Plexiglas chamber at normal air temperature (sham control).

Histochemistry

Injury to different brain areas was determined from triphenyltetrazolium chloride (TTC, Sigma, St. Louis, MO, USA) staining of brain sections (2 mm) collected at 24 post-HI and from Nissl-stained brain sections and obtained at 7 d post HI as described previously (Hossain et al., 2004; Thatipamula et al., 2015). Quantitative morphometric analysis of injury volumes were determined using the computer-assisted image analysis software package Microcomputer Imaging Device (MCID) of Imaging Research (Brock University, St. Catharines, Ontario, Canada) according to our established methods (Hossain et al., 1998). For Nissl-stained sections, brain injury was assessed by histologic analysis of striatum and dorsal hippocampus. Serial 25 µm coronal sections were cut with a Cryostat (Microma, Heidelberg, Germany) and stained with 0.5% Cresyl violet. For each animal, the cross-sectional area of striatum and hippocampus both ipsilateral and contralateral sides were measured using MCID image analysis.

For TTC staining, a subset of animals from sham controls and HI groups were sacrificed by decapitation at indicated times post-HI to determine cerebral infarctions as described previously (Hossain et al., 2004). The area of infarction was visualized with a digital scanner (HP Scanjet G4010) and quantified by MCID analysis to determine infarct volumes. The average values of percent damage were determined for each structure and animal.

Mouse Embryonic Cortical Cultures and OGD

Primary cortical neuronal cultures were prepared from embryonic day 16 (E16) WT C57BL/6 mice as described previously (Russell et al., 2011). Primary cortical neurons

were grown in a culture medium consisting of Neurobasal™ medium (Cat # 21103049, Invitrogen, Gaithersburg, MD, USA), 2% B27 supplement (Cat # 17504044, Invitrogen), 2-mM L-glutamine (Cat # 35050061, Thermo Fisher Scientific, Waltham, MA, USA), and 1% penicillin–streptomycin (Cat # 15140122, Thermo Fisher Scientific) as described (Russell et al., 2011; Al Rahim et al., 2013). Experiments were conducted at DIV 12, when cultures consisted primarily of neurons (>95% MAP-2 immunoreactive cells) (MAP-2, Cat # MAB3418, RRID: AB_94856, Chemicon, Temecula, CA, USA). Oxygen glucose deprivation (OGD) exposure was performed as described previously (Russell et al., 2011; Al Rahim et al., 2013).

Transient Transfection of Primary Cortical Neurons

Primary cortical neurons were isolated from E16 embryonic mouse brain cerebral cortex and transfected by nucleofection system using Mouse Neuron Nucleofector kit (Cat # VPG-1001, Amaxa, Inc.; Russell et al., 2011). Primary neuronal cells in a suspension containing 5×10^6 cells were mixed with 2 µg of either DsRed2 control vector or pDSRed2-Mito vector DNA (Cat #632421, Clontech, Mountain View, CA, USA). Following nucleofection, cells were plated on coverslips at a density of 2.5×10^5 cells/cm² area.

Immunofluorescence

To assess the distribution of NP1 protein in different brain regions and sub-regions (e.g. hippocampal CA1, CA3 and dentate gyrus) representative coronal brain sections (20 µm) were subjected to immune-staining and analyzed by fluorescence microscopy as described previously (Hossain et al., 2004; Thatipamula et al., 2015). Representative coronal brain sections (20 µm) from control and HI animals were immunostained as described previously (Hossain et al., 2004; Al Rahim and Hossain, 2013). Mouse monoclonal anti-NP1 (1:200) (Cat #610369, RRID: AB_397754, BD Transduction Laboratories, Temecula, CA, USA) was used as the primary antibody, while donkey anti-mouse, anti-rabbit Alexa fluor 488 (green) and 568 (red) are the secondary antibodies (Cat #R37114, RRID: AB_2556542; Cat #A10042, RRID: AB_2534017, Thermo Fisher Scientific). For double label immunostaining of NP1 (Cat #610369, RRID: AB_397754, BD Transduction Laboratories) and HKII (1:200, Cat #2024, RRID: AB_2116996, Cell Signaling, Beverly, MA, USA), brain sections or primary neuronal cultures were stained with anti-NP1 and anti-HKII followed by appropriate secondary antibodies. Immunofluorescence was visualized using an inverted fluorescence microscope (Olympus IX51 fitted with DP2-DSW-V3.2 application software)

at 10 X and ZEISS Axioimager M2 (AxioVision SE64 Rel.4.8.1 application software) at 100 X magnification.

Preparation of Cytosolic and Mitochondrial Fractions

Subcellular fractionation was performed using cortical tissues from sham control and HI animals (WT and NP1-KO) as described previously (Russell et al., 2011; Al Rahim et al., 2013). Briefly, the cortices were collected and placed in 10 volumes of ice-cold homogenation buffer (250 mM sucrose, 10 mM HEPES, 1 mg/ml BSA, 0.5 mM EDTA, 0.5 mM EGTA) supplemented with protease and phosphatase inhibitor cocktails (Cat #C134544, Calbiochem, San Diego, CA, USA). Tissues were homogenized using a hand-held homogenizer by eight strokes and centrifuged at 2000 g for 3 min. The pellet (P1) is the nuclear fraction. The post-nuclear supernatant (S1) was centrifuged at 12,000 g for 8–10 min at 4°C for the cytosolic and mitochondrial fraction. The supernatant was used as the crude cytosolic fraction. The pellet was washed with sucrose buffer (in mM: 320 sucrose, 3 CaCl₂, 2 Mg-acetate, 0.1 EDTA, 10 Tris-HCl), and further centrifuged at 12,000 g for 10 min. The pellet containing the mitochondrial fraction was resuspended in sucrose buffer supplemented with protease and phosphatase inhibitor cocktails. To confirm the separation of cytosolic and mitochondrial fractions, blots were stripped and incubated with β -Actin (Cat #A5441, RRID: AB_476744, Sigma) and prohibitin (Cat #PA5-17325, RRID: AB_10977876, Thermo Fisher Scientific), respectively, which also served as loading controls.

Immunofluorescence of Neuronal Cultures

After plating the transfected cortical cells on glass coverslips, cells were exposed to OGD at DIV 12 for 1–2 h. Following exposure, the medium was removed, and the cells were rinsed in PBS and were fixed in 4% paraformaldehyde in PBS containing 2% sucrose for 15 min. Cells were later permeabilized and blocked in block solution (PBS containing 5% donkey serum) for 60 min. Subsequent incubation with NP1 antibody (1:200, Cat #610369, RRID: AB_397754, BD Transduction Laboratories) and HKII (1:250, Cat #2024, RRID: AB_2116996, Cell Signaling) was performed in blocking solution overnight followed by washes in PBS. Neurons were then stained with appropriate secondary antibodies (Cat #R37114, RRID: AB_2556542; Cat #A10042, RRID: AB_2534017, Thermo Fisher Scientific) for 1 h at RT. After PBS washes, cells were mounted with Prolong Gold Antifade (Cat #P36935, Thermo Fisher Scientific).

SDS-PAGE and Western Blot Analyses

Western blotting was performed with standard methods as described previously (Al Rahim et al., 2009, 2013). Whole cell lysates or the proteins extracted from brain tissue were subjected to Western blot analysis. Protein concentrations were measured following bicinchoninic acid (BCA) assay. Blots were probed with primary antibodies for NP1 (1:1000, Cat #610369, RRID: AB_397754, BD Transduction Laboratories), MitoBiogenesis Western Blot Cocktail (antibodies include SDH-A, mtCOX-1 and β -Actin) (1:1000, Cat #ab123545, RRID: AB_2756817, Abcam), Hexokinase II (1:1000, Cat #2024, RRID: AB_2116996, Cell Signaling), HSP60 (1:1000, Cat #4877, RRID: AB_2233307, Cell Signaling), COX-IV (1:1000, Cat #4850, RRID: AB_2085424, Cell Signaling), TFAM (1:500, Cat #8076, RRID: AB_10949110, Cell Signaling), PGC-1 α (1:500, Cat #ab54481, RRID: AB_881987, Abcam), and β -actin (1:5000, Cat #A5441, RRID: AB_476744, Sigma). After visualizing the blots with enhanced chemiluminescence, digitized images were quantified using NIH ImageJ software.

Measurement of Intracellular ATP

Intracellular ATP levels were determined by using ATPlite, a luminescence-based kit (Cat #6016943, PerkinElmer, Waltham, MA, U.S.A.). Cellular extracts were prepared from cortical neuronal cultures exposed to OGD as indicated in the respective figure by adding an appropriate volume of mammalian lysis buffer. ATP quantification in the extracts was performed according to the manufacturer's instructions. Chemiluminescence was measured in luminometer (Tristar LB 941, Berthold Technologies, Oak Ridge, TN, USA). Results were normalized according to the protein content of the extracts.

RNA Isolation and Real-Time PCR

Total RNA was isolated by RNeasy kits (Cat #74104, Qiagen, Valencia, CA, USA) according to the manufacturer's instructions. cDNA was synthesized from 1 μ g of purified total RNA using iScriptTM cDNA Synthesis Kit (Cat #1708890, Bio-Rad laboratories, Richmond, CA, USA). Quantitative real-time PCR was performed in triplicate by using iQ SYBR Green Supermix (Cat #1708880, Bio-Rad laboratories) on CFX96TM Real-Time System (Bio-Rad laboratories) as described previously (Al Rahim et al., 2013). The mRNA level was normalized by housekeeping gene HPRT. The primers set used were: for NP1, 5'-GCT GCG AGA GCC AGA GCA CC-3' (sense) and 5'-TTG CCC GAG TTG GCT GAG CG-3' (anti-sense), for TFAM, 5'-AGT TCA TAC CTT CGA TTT TC-3' (sense) and 5'-TGA CTT GGA

GTT AGC TGC-3' (anti-sense), for PGC-1, 5'-CAC GCA GCC CTA TTC ATT GTT CG-3' (sense) and 5'-GCT TCT CGT GCT CTT TGC GGT AT-3' (anti-sense), and for HPRT were 5'-CCT GGC GTC GTG ATT AGT GAT G-3' (sense) and 5'-CAG AGG GCT ACA ATG TGA TGG C-3' (anti-sense).

Mitochondrial DNA Measurement

The amount of mitochondrial DNA relative to nuclear genomic DNA in control and HI cortical tissue was determined by quantitative real-time PCR using primers 5'-GTTCGCAGTCATAGCCACAGCA-3' (sense) and 5'- AACGATTGCTAGGGCCGCGAT-3' (antisense) for cytochrome b (mitochondrial) and 5'-CTCAAGGT CGTGCGTGCCTG-3'(sense) and 5'-TGGCTTT CTCTTTCCTTCTC-3'(antisense) for RPL13A (nuclear). Relative mitochondrial DNA levels were calculated as described previously (Sharma et al., 2014).

Coimmunoprecipitation

Bax6A7 immunoprecipitation was performed in protein extracts from either brain cortical region or cortical neurons exposed to OGD. For brain cortical extraction, cortices were homogenized in 10 volumes of immunoprecipitation buffer (in mM: 50 Tris-HCl, 100 NaCl, 2 CaCl₂, 1% Triton X-100) containing 1X protease inhibitor cocktail set I, and phosphatase inhibitor cocktail II (Calbiochem; Al Rahim et al., 2013). For cortical cultures, cells were washed with PBS on ice, and lysed in immunoprecipitation buffer. Protein concentrations were measured following BCA assay. Fixed amount of proteins (750 µg of cell lysates, and 1 mg of cortical tissue homogenate) were subjected to immunoprecipitation by incubating overnight with Bax6A7 (1:100, Cat #ab5714, RRID: AB_305079, Abcam) at 4°C. Then, 20 µl of protein A/G-agarose conjugated beads was added to each sample and incubated for 2–4 h at 4°C. The beads were collected, washed, and boiled for 3 min in 50 µl of 1X electrophoresis sample buffer followed by Western blot analysis.

Statistical Analysis

Statistics were performed using GraphPad Prism software, Version 8. Shapiro-Wilks normality tests were used to assess data distribution. All data exhibited a normal/Gaussian distribution. Statistical analyses involving multiple groups were done by one-way ANOVA, followed by Bonferroni/Dunn post hoc test. Significance level was assigned at $P < 0.05$. All results are presented as means \pm SD.

Results

Hypoxia-Ischemia Induces NP1 Protein Expression, and Promotes Its Mitochondrial Accumulation

We have shown previously induction of NP1 in hypoxic-ischemic neuronal death (Hossain et al., 2004; Russell et al., 2011; Al Rahim et al., 2013), and NP1 induction is an early event contributing to the death program. To examine the early effects of HI in relation to NP1 induction and brain injury, neonatal mice were subjected to HI, and cerebral cortices were collected at 6, 12 and 24 h after the insult for immunostaining and biochemical experiments (Figure 1). First, brain injury was assessed from TTC-stained brain sections (20 µm) (Figure 1A), and by Nissl staining of coronal brain sections showing evidence of enhanced ipsilateral cortical brain injury at 7d post-HI (Figure 1B). Next, we performed immunofluorescence staining of brain sections from WT neonatal mouse HI brains for assessment of NP1 induction. Previously, we have reported that NP1 is induced in neurons before actual tissue loss (Al Rahim et al., 2013). We collected the images from the ipsilateral frontal and parietal cortex, specifically the cortical penumbra regions, since NP1 staining is more intense in the ischemic penumbra where neuronal death is slowly developing (Thatipamula et al., 2015). Fluorescence microscopy showed enhanced NP1-specific immunoreactivity in the ipsilateral cortex 24 h after HI onset (Figure 1C). No induction in NP1-immunoreactivity was observed in the contralateral side of the brain. We have reported previously that NP1 is not expressed/induced in astrocyte cells following HI; and that NP1 expression/induction is exclusively neuronal (Thatipamula et al., 2015). Further analysis of brain sections by fluorescence microscopy revealed intense NP1-specific fluorescence localized in the perinuclear regions of individual neurons in the cortical regions (inset) compared to the sham controls (Figure 1C). Quantitative assessment of NP1 protein levels by Western blot analyses of the cortical tissue homogenate showed a time-dependent induction (2-3 folds) of NP1 levels (Figure 1D). Induction of NP1 was observed as early as 6 h which reached maximum at 24 h, examined; corroborating the induction of NP1 in the cortex following HI.

Previously, we have reported that NP1 overexpression facilitates mitochondria-mediated neuronal injury (Russell et al., 2011; Al Rahim et al., 2013). To investigate the brain injury mechanism more in-depth, we analyzed the subcellular distribution of NP1 in developing cerebral cortex following HI. As shown in Figure 2A, HI caused a substantial increase in the amount of NP1 protein in mitochondrial fraction as compared to that of sham controls. The accumulation of NP1 in mitochondria was evident as early as 12 h after HI and increased further at 24 h post-

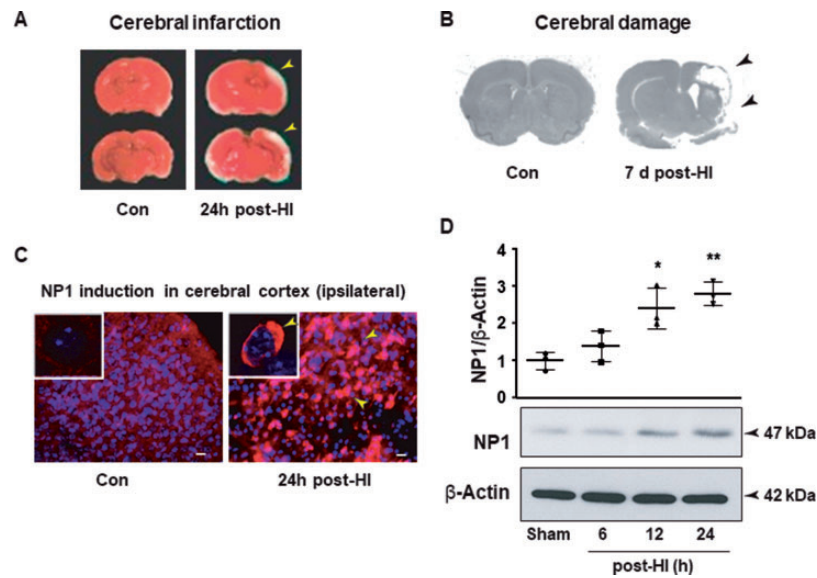


Figure 1. NP1 Is Induced in the Cortex Following Hypoxia-Ischemia. A: TTC-staining of brain sections (2 mm) showed marked infarction (white areas denoted by yellow arrowhead) in the right cerebral hemisphere as compared to the sham controls. Con is sham control; HI is hypoxia-ischemia. B: Nissl-stained brain sections of sham control (left panel) and HI (right panel) mice. HI caused an injury in ipsilateral-cortical areas, but no injury/tissue loss (neuroprotection) in the sham control. Representative images are shown. C: Representative coronal brain sections (20 μ m) of ipsilateral sides of cortex from 24 h post-HI were analyzed for NP1-specific immunofluorescence (red). Scale bars: 100 μ m. Yellow arrowheads specify NP1 immunostaining, and blue is DAPI. D: Representative Western blots showing NP1 protein levels at different times (6-24 h) following HI. Quantitative densitometry values normalized to β -Actin are also shown above the respective NP1 bands. Values are mean \pm SD ($n = 3$, * $p < 0.05$ and ** $p < 0.01$, one-way ANOVA followed by Bonferroni/Dunn post hoc test).

HI. In comparison, increase in NP1 in cytosolic fractions occurred at earlier time-points, beginning at 6 h, reaching peak at 12 h followed by a decrease in protein levels at 24 h post-HI. This result indicates that the amount of NP1 induced following HI remains in the cytosol at the early stage and subsequently translocates in a large proportion to mitochondria during the later time periods post-HI. To further substantiate the mitochondrial localization of NP1, primary cortical cultures were transfected with DsRed2 control vector and pDSRed2-Mito vector DNA, and cortical cultures were exposed to 2 h oxygen glucose deprivation (OGD) at 12 days *in vitro* (DIV) (Figure 2B). This vector is designed for red fluorescence labeling of mitochondria with the mitochondrial targeting sequence from subunit VIII of cytochrome c oxidase (Mito; Hsu and Youle, 1998) that targets to the host cell's mitochondria. Overlapped immunofluorescence images of MtdsRed (red) and NP1 (green) further confirmed a marked increase in NP1 localization into the mitochondria (yellow) following OGD exposure as compared to normoxia control neurons (Figure 2B).

Hypoxia-Ischemia Enhances Mitochondrial DNA Content, Expression of Mitochondrial Proteins and Proteins Encoded by Mitochondrial DNA

To correlate between NP1 induction and mitochondria-mediated neuronal death, we have examined the

functional response of mitochondrial (mt) - and nuclear (n)-DNA following HI. Mitochondrial DNA expression was analyzed in the entire ipsilateral cortex by RT-qPCR (Chen et al., 2001) using mouse genomic DNA as internal amplification standard and expressed as ratio of mitochondrial:nuclear DNA as described previously (Sharma et al., 2014). The mtDNA content was increased significantly ($p < 0.01$) as early as 6 h post-HI and remained increased but to a lesser extent up to 24 h post-HI examined (Figure 3A). We presume that the changes are confined to the area of the lesion, especially the penumbra areas. It is important to mention here that we did not observe any changes of mtDNA content in the contralateral cortex (data not shown), and that nuclear DNA remained unchanged as well.

Next, we determined the expression of two target proteins; one, subunit I of complex IV (COX-1), which is mtDNA-encoded (mtCOX-1) and the subunit of succinate dehydrogenase A (SDH-A), which is nDNA-encoded (nSDH-A), by Western blot analysis and normalized with β -Actin (Figure 3B). The antibody cocktail used detects all three proteins simultaneously on the same membrane. The expression of nDNA-encoded protein SDH-A remained unchanged following HI as compared to sham animals (Figure 3B.1). In contrast, there was a HI-time dependent increase in expression of mtDNA-encoded mtCOX-1 beginning at 6 h and remained elevated up to 24 h post-HI ($p < 0.05$) compared to sham

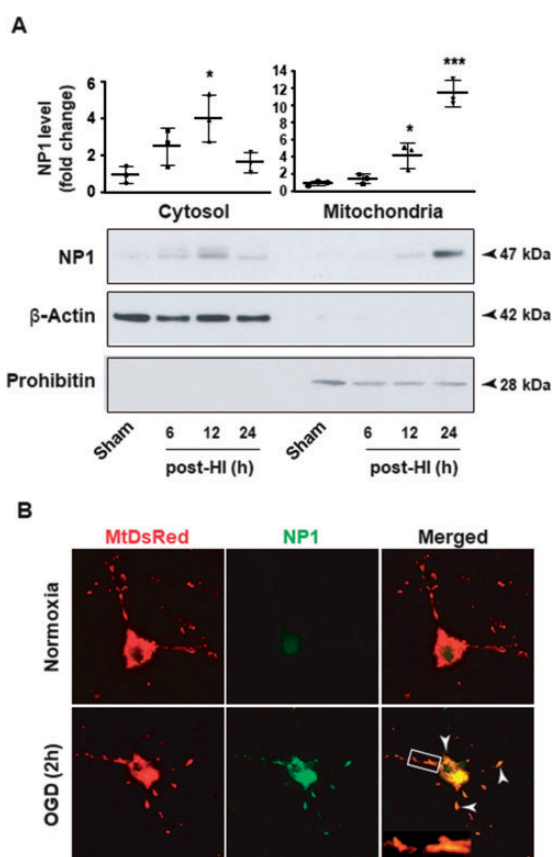


Figure 2. Hypoxia-Ischemia Ensuers Increased Accumulation of NP1 in Mitochondria. **A:** Subcellular fractionation of cortical tissue extracts was performed following HI. Western blot analyses showed increased mitochondrial accumulation of NP1 after HI. Prohibitin and β -actin were used as a control for purity of the mitochondrial and cytosolic fractions, respectively, which also served as loading controls. Representative blots are shown. Normalized quantitative densitometry values are also shown. Values are mean \pm SD ($n = 3$, * $p < 0.05$ and *** $p < 0.001$, one-way ANOVA followed by Bonferroni/Dunn post hoc test). **B:** Representative images of mitochondria labeled with MtDsRed (red) and immunocytochemistry of NP1 (green) in cortical neuronal cultures after 2 h of OGD exposure. Merged images of MtDsRed and NP1 confirm mitochondrial accumulation of NP1 (yellow; shown by white arrows). Exposure to OGD increased NP1 immunofluorescence in mitochondrial regions. Scale bars: 20 μ m. An inset with magnification is also shown.

control (Figure 3B.2). The observed increase in mtCOX-1 suggests that mtDNA is more responsive to HI compared to nDNA under similar conditions.

To gain additional evidence for mitochondrial response in the event of HI, we examined the expression of proteins that are normally enriched in mitochondria. Heat shock protein 60 (HSP60) is a protein predominantly located in mitochondria, with only 15–20% normally found in the cytosol (Gupta and Knowlton, 2002). We found increased expression of HSP60 in the cortex following HI (Figure 3C). The HSP60 protein levels were

enhanced at 6 h, which sustained for, at least, 24 h after HI (Figure 3C.1). Next, we asked whether an increase in HSP60 was simply a manifestation of the HI-induced stress effect or an indication of an augmented mitochondrial biogenic program. We examined the expression of the mitochondrial-specific protein, mitochondrial respiratory protein cytochrome C oxidase subunit IV (COX-IV). A similar time-dependent increase of COX-IV protein with maximum increase at 24 h post-HI was observed in the ipsilateral cortex (Figure 3C.2). Our results indicate that mitochondrial compensatory mechanism involving mitochondrial biogenic program may play a role at the early stage of HI.

Hypoxia-Ischemia Triggers Neuronal Injury by Enhancing NP1 Interaction With Active Bax and HKII

Previously, we reported that interaction of NP1 with the pro-death proteins Bax and Bad was associated with a mitochondrial release of Cyt C and activation of caspase-3 (Al Rahim et al., 2013). To become active, Bax undergoes a conformational change in the N terminus that exposes an epitope comprising amino acids 13–19 known as 6A7 (Hsu and Youle, 1998). Here, we have examined direct interaction of NP1 with activated Bax in cerebral cortex following HI and in primary cortical neurons exposed to OGD (Figure 4). We performed immunoprecipitation studies using an antibody that recognizes the 6A7 epitope to distinguish active Bax from the other non-active forms (Hsu and Youle, 1998). NP1 was co-immunoprecipitated with active Bax[6A7] in homogenates from HI cortical tissue and increased precipitation of NP1 was observed following HI (Figure 4A). Similarly, co-immunoprecipitation of active Bax and NP1 was detected in lysates of primary cortical cultures and that 2 h of OGD exposure enhanced the amount of NP1 immunoprecipitated with active Bax (Figure 4B). We did not observe any changes in the expression of Bax at 2 h of OGD (Figure 4B, inputs); however, the expression of the protein started declining as early as 4 h of OGD exposure (Al Rahim et al., 2013).

It has been reported that mitochondrial binding of HKII promotes cell survival by inhibiting Bax-induced Cyt C release and apoptotic cell death (Pastorino et al., 2002). Our findings above confirmed the interaction between NP1 and active Bax. However, how HKII antagonizes Bax-mediated apoptosis is presently debated. Here, we asked if NP1 interacts with mitochondrial HKII, and whether OGD-induced NP1 interaction with Bax[6A7] (NP1-Bax6A7) causes HKII detachment from mitochondria. Cortical neurons were transfected with mitochondrially targeted MtDsRed, and OGD exposed cells were immunostained with HKII antibody (Figure 4C). Fluorescence microscopy revealed that HKII is localized in mitochondria (mtHKII) during

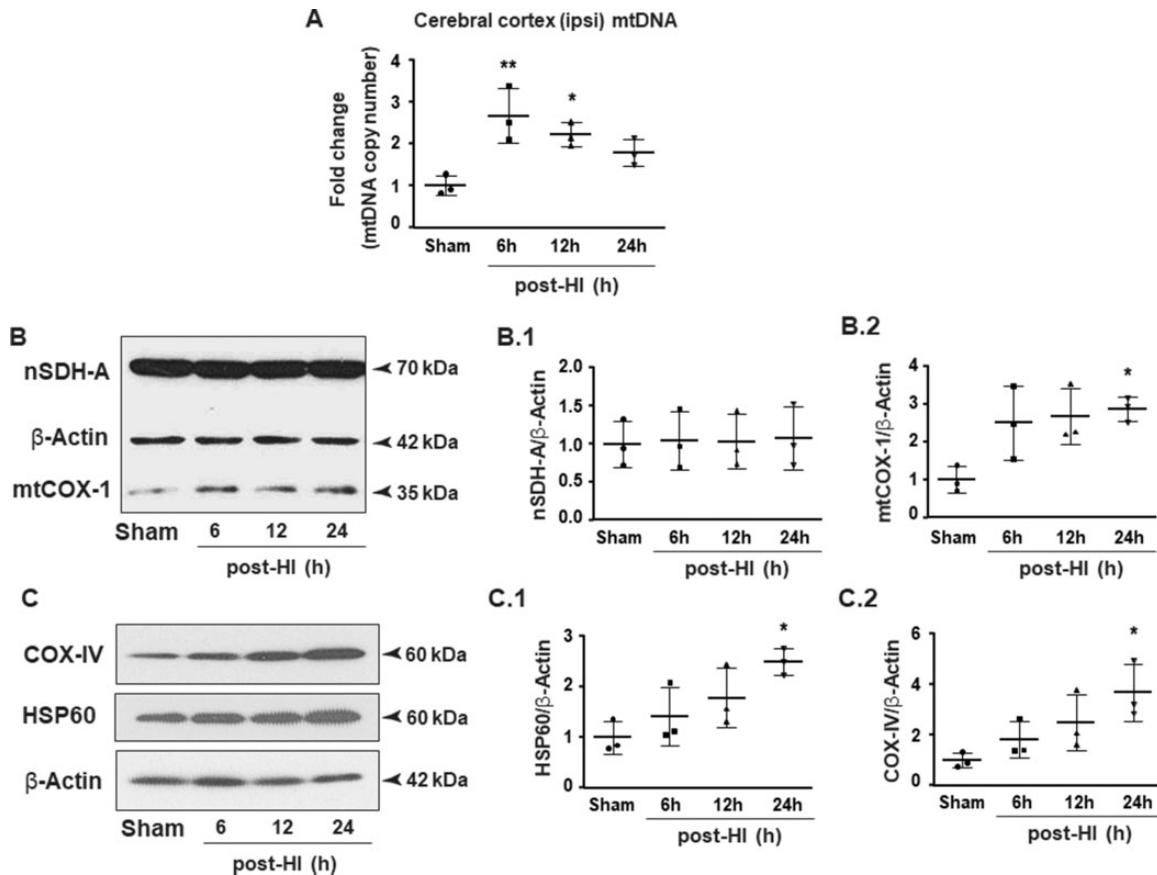


Figure 3. Hypoxia-Ischemia Augments Expressions of Mitochondrial DNA and Mitochondrial Proteins. A: The ratio of mitochondrial: nuclear DNA was determined by quantitative real-time PCR. The fold change of mtDNA over sham control showed significantly increased mtDNA at early periods (6-24 h) of HI. Results are mean \pm SD ($n = 3$, * $p < 0.05$ and ** $p < 0.01$, one-way ANOVA followed by Bonferroni/Dunn post hoc test). B: HI induces protein expression encoded by mitochondrial DNA. Using a Mitochondriogenesis WB Antibody Cocktail, we found that mtDNA-encoded protein mtCOX-1 (B.2), but not nDNA-encoded protein SDH-A (B.1), expression was enhanced in response to HI. The antibody cocktail, which simultaneously detected expressions of three different proteins, also included β -Actin that served as an internal control. Representative blots are shown. C: Representative WB images showing expressions of mitochondrial-specific protein, COX-IV; and mitochondrial-enriched protein, HSP60 at different time-points following HI. After HI, both HSP60 (C.1) and COX-IV (C.2) proteins were increased which sustained for 24 h, examine. Quantitative densitometry values normalized to β -actin are shown above the corresponding blots. Values are mean \pm SD ($n = 3$, * $p < 0.05$, one-way ANOVA followed by Bonferroni/Dunn post hoc test).

normoxia as evidenced by clusters of HKII that colocalized with MtDsRed-labeled mitochondria (yellow). However, OGD exposure caused significant mtHKII dissociation as demonstrated by substantial reduction in HKII-specific immunofluorescence colocalized with MtDsRed (Figure 4C, bottom panel). Next, we examined the interaction between NP1 and HKII by performing double immunostaining with respective antibodies. Overlapping images showed NP1 co-localization with HKII, and that 1 h of OGD exposure substantially enhanced NP1-HKII interaction (yellow) (Figure 4D). Our results suggest that NP1 interaction with HKII could be an early event that initiated the observed dissociation of HKII from mitochondria at a later time following OGD. To further confirm the NP1-HKII interaction and HKII detachment from the mitochondria we perform subcellular fractionation of control and

OGD-exposed cortical neurons. Western blot analysis showed presence of NP1 and HKII in cytoplasmic fraction at the initial 1 h of OGD exposure, but the HKII-specific immunoreactive band disappeared at 2 h of OGD with concomitant increase of NP1 in mitochondrial fraction (Figure 4E). The specificity of NP1-HKII interactions was further demonstrated by pretreatment of cells with GSK-3 β inhibitor SB216763, which inhibited NP1 induction as reported previously (Russell et al., 2011; Al Rahim et al., 2013). We found that the presence of intense HKII immunoreactive band was apparent in mitochondrial fraction with simultaneous disappearance of NP1 band following inhibition of GSK-3 β , under the conditions we previously reported inhibition of NP1 induction and neuroprotection (Russell et al., 2011; Al Rahim et al., 2013). To further validate our *in vitro* findings of NP1 interaction with HKII, we performed

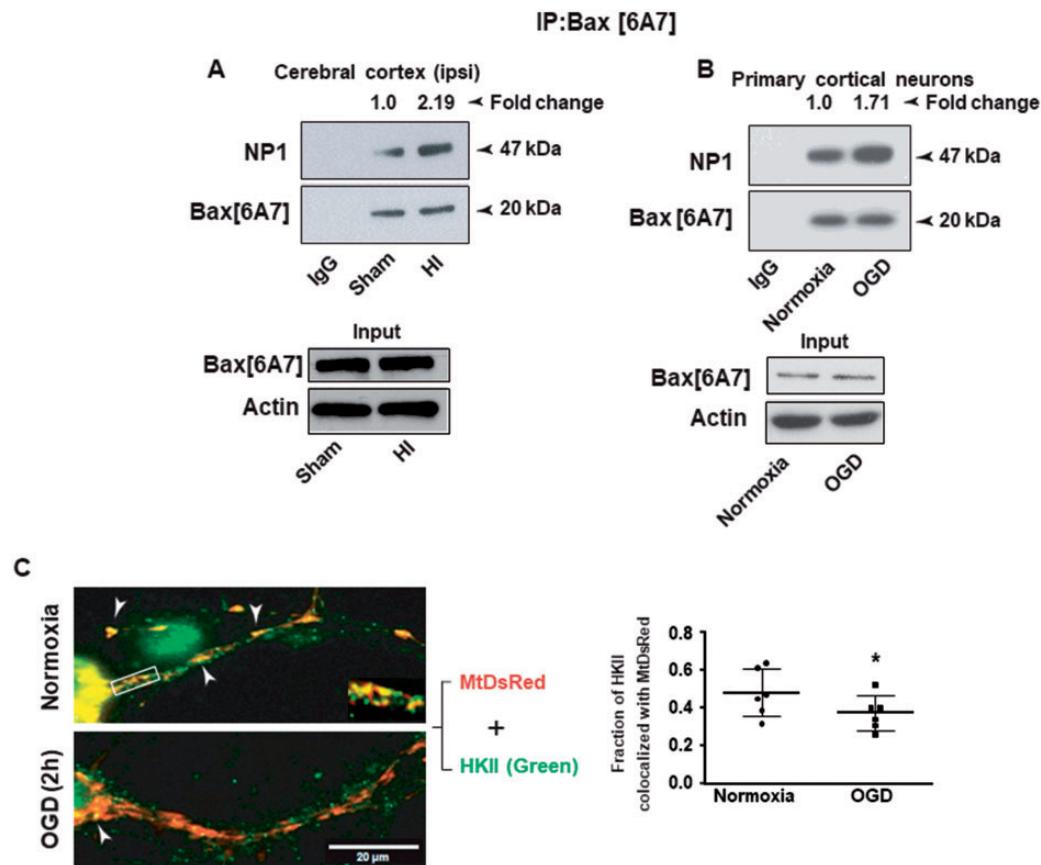


Figure 4. Hypoxia-Ischemia Enhances Interactions of NP1 With Active Bax (Bax6A7) and HKII Dissociation From Mitochondria. SDS-PAGE and immunoblotting of active Bax immunoprecipitates from 24 h post-HI cortical tissue homogenate (A) and from 2 h OGD-exposed primary cortical neuronal lysates (B) showed increased NP1 co-precipitation (2-fold) with active Bax following HI and OGD relative to respective controls. IgG immunoprecipitates showed no evidence of NP1-, and active Bax-specific bands. Representative blots are shown. Quantitative densitometry values are shown above the respective Bax6A7 bands. C: Representative images of mitochondria labeled with MtDsRed (red) and immunocytochemistry of HKII (green) after 2 h of OGD exposure. Merged image of MtDsRed and HKII revealed presence of HKII in mitochondria (yellow) shown by white arrows. In contrast, exposure to OGD decreased HKII localization in mitochondria. Graphs show fraction of HKII colocalized with MtDsRed following Mander's colocalization coefficients. Data are mean \pm SD ($n = 6$, $*p < 0.05$, two-tailed t -test). D: Representative immunofluorescence images of NP1 (red) and HKII (green). Merged image showed enhanced NP1-HKII interaction (yellow) following 1 h of OGD, as evidenced by increased co-localizations of the proteins (white arrows). Scale bars: 20 μ m. Graphs show fraction of HKII colocalized with NP1 following Mander's colocalization coefficients. Data are mean \pm SD ($n = 6$, $**p < 0.01$, two-tailed t -test). E: Subcellular fractionations of control normoxia and OGD-exposed primary cortical cultures followed by western blotting showed mitochondrial accumulation of NP1 with simultaneous decrease of mtHKII protein levels at 2 h of OGD exposure. Pretreatment with GSK-3 inhibitor SB216763 (10 μ M) showed conjoint decrease of mitochondrial NP1 and increase of mtHKII protein levels, further confirming mtHKII detachment from mitochondria with NP1 accumulation. Representative blots are shown. F: Fluorescence of brain sections immunostained with NP1 and HKII antibodies revealed NP1: HKII colocalization in ipsilateral cerebral cortex at 6-24 h post-HI compared to that in sham controls.

dual immunofluorescence staining of brain sections from sham control and HI animals using NP1- and HKII-specific antibodies. Fluorescence microscopy of cortical brain regions revealed intense co-localization of NP1 and HKII at 24 h post-HI as compared to sham controls (Figure 4F). Our results clearly demonstrate that NP1 interacts with mitochondrial HKII at the early period post-HI, which in turn causes dissociation of HKII from mitochondria resulting in neuronal death in HI brain injury.

Inhibition of NP1 Expression Reverses OGD-Induced HKII Displacement From Mitochondria and Loss of Intracellular ATP Content

Here, we examined whether inhibition of NP1 expression could prevent OGD-induced HKII dissociation from mitochondria by measuring HKII in cytosolic and mitochondrial compartments of OGD exposed NP1^{-/-} cortical neurons. Our results showed that in absence of NP1 expression in NP1^{-/-} cortical neurons, almost all of the

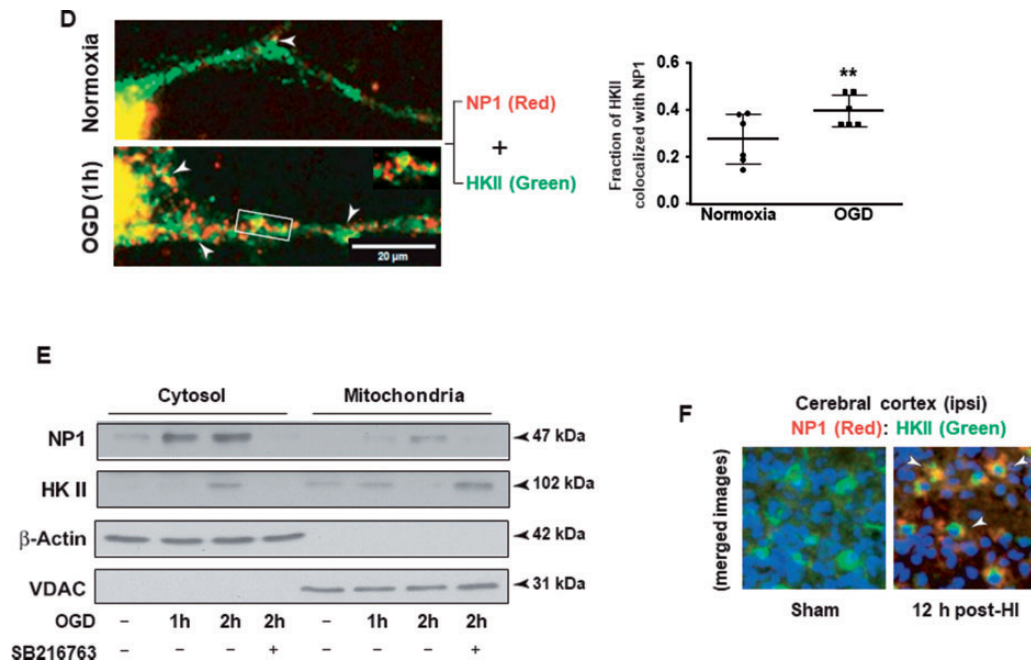


Figure 4. Continued

HKII protein remained mitochondria bound even at 2 h of OGD (Figure 5A) in stark contrast with WT neurons under similar OGD conditions (Figure 4E). Furthermore, pretreatment with GSK-3 inhibitor SB216763 also showed a tendency of higher HKII presence in mitochondrial fraction (Figure 5A). Next, to directly demonstrate the link between NP1 induction and mtHKII displacement, we exposed MtDsRed-transfected NP1^{-/-} cortical cultures to identical OGD condition (2 h). In contrast to WT neurons (Figure 4C), merged images revealed that OGD could not cause mtHKII dissociation in NP1^{-/-} neurons (Figure 5B), suggesting NP1 gene deletion prevents OGD-evoked mtHKII detachment from mitochondria (Al Rahim et al., 2013).

Next, to demonstrate the specific interaction of NP1 with mtHKII and HKII detachment from mitochondria, total cellular lysates from the control and OGD exposed WT cortical neurons were immunoprecipitated with anti-HKII antibody. At 1 h of OGD, the physical association of NP1 and mtHKII was evident, but there was no interaction between NP1 and HKII at 2 h of OGD (Figure 5C). Interestingly, pretreatment with GSK-3 inhibitor also showed the absence of NP1-HKII association at 1 and 2 h of OGD, confirming HKII detachment from mitochondria (Figure 5C). Loss of ATP production constitutes a critical effector mechanism in cell commitment to death following the loss of mitochondrial membrane integrity (Halestrap et al., 2000; Hagberg, 2004). To examine that notion, we measured the levels of intracellular ATP content in cortical neurons under similar

conditions. We found that OGD drastically decreased the ATP levels in the neurons compared to normoxia, while pretreating cells with GSK-3 inhibitor significantly improved the intracellular ATP content following OGD (Figure 5D), indicating the role of NP1 in disrupting mitochondrial energy metabolism system leading to neuronal death. However, GSK3 inhibitor, SB216763, alone did not cause any change to the ATP content of the cells.

Deletion of NP1 Gene Supports Augmented Expression of Mitochondrial Biogenesis Factors in Response to HI

Enhanced mitochondrial biogenesis in neurons has been reported after transient hypoxic-ischemic brain injury (Gutsaeva et al., 2008; Yin et al., 2008). Our present results showing increased mitochondrial protein HSP60 and COX-IV expression following HI (Figure 3C) lends additional credence to this possibility. However, evidence in support of mitochondrial biogenesis in the event of delayed neurodegeneration remains incomplete, and mechanisms underlying reduction in the mitochondrial biogenic capacity following such insult is unknown. Cerebral cortices were collected at 6, 12, 24, 48 and 72 h after HI to examine mRNA expression levels of NP1, and two transcription factors, TFAM and PGC-1 α considered essential for mitochondrial biogenesis (Figure 6). We found a temporal increase in the expression of NP1 mRNA levels, which remained elevated until 72 h after HI, examined (Figure 6A). However, the mRNA levels of TFAM and PGC-1 α increased initially

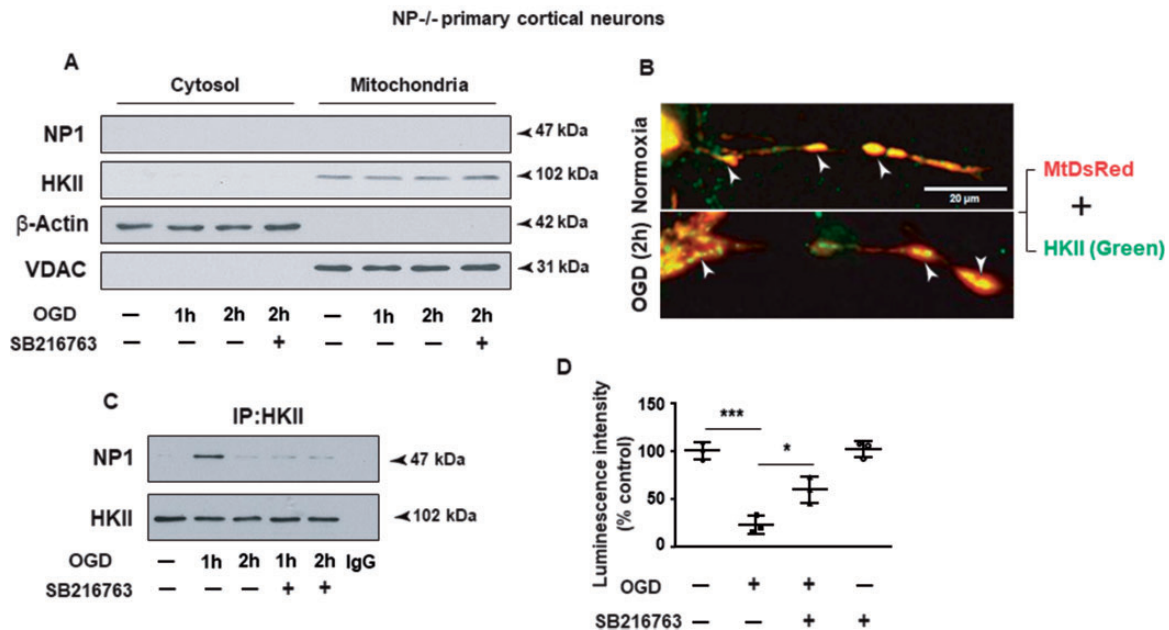


Figure 5. Knockdown of NP1 Expression Blocks OGD-Induced Mitochondrial HKII Detachment and Loss of Intracellular ATP Content. NP1^{-/-} cortical cultures were exposed to OGD (1–2 h), and a subset of cultures were pretreated with SB216763 (10 μM for 12 h), a GSK-3 inhibitor. **A:** Western immunoblotting shows intense mtHKII protein bands in the mitochondrial fraction after in the absence of NP1 protein in NP1 null cells, also confirming the knockout status of cortical cultures. Pretreatment with GSK-3 inhibitor SB216763 as in Figure 4, further increased the HKII protein levels in the mitochondrial fraction. **B:** Representative images of mitochondria labeled with MtdsRed (red) and immunocytochemistry of HKII (green) after 2 h of OGD exposure in NP-KO cortical cultures. Merged images of MtdsRed and HKII show mitochondrial HKII (yellow), shown by white arrows. Exposure of NP^{-/-} cultures to OGD did not cause any noticeable displacement of HKII from mitochondrial regions. Scale bars: 20 μm. **C:** Wild type cortical lysates were immunoprecipitated with anti-HKII antibody and subjected to Western blot analysis. Results show association of NP1 with HKII at 1 h of OGD which disappeared at 2 h of exposure, suggesting NP1-mtHKII association. Similarly, pretreatment of GSK-3 inhibitor blocked NP1 interaction with mtHKII. **D:** GSK-3 inhibitor pretreatment significantly improved OGD-evoked loss of intracellular ATP content as measured in respect to luminescence intensity. Values are presented as mean ± SD. (n = 3; *p < 0.05 and ***p < 0.001, one-way ANOVA followed by Bonferroni/Dunn post hoc test).

until 24 h following HI in WT brains, which was reduced to below the control levels at 48–72 h post-HI (Figure 6B and C, left panels). To specifically identify the effects of NP1 mRNA expression on the regulation of mitochondrial biogenesis following HI, we used NP1-KO animals and subjected them to identical conditions. Most strikingly, our results showed a persistent increase in the expressions of both TFAM and PGC-1α mRNA throughout the 6–72 h post-HI time points (Figure 6B and C, right panels).

To gain additional evidence in support of enhanced expression of transcription factors PGC-1α and TFAM, we evaluated respective protein levels by Western blot analysis (Figure 7). Similar to the mRNA expression, the NP1 protein levels increased significantly up to 72 h post HI (Figure 7A). The proteins levels of TFAM (Figure 7B) and PGC-1α (Figure 7C) were also increased initially until 24 h, which was then reduced significantly to the control levels at 48–72 h post-HI in WT cortex (left panels). In contrast, the TFAM and PGC-1α protein levels remained increased up to 72 h post HI in the

NP1-KO brains (Figure 7B and C, right panels). Together, our results suggest that NP1 gene deletion resulted in augmentation of mitochondrial biogenesis program in response to HI; thereby facilitating the mitochondrial compensatory mechanisms under the conditions we observed neuroprotection against hypoxic-ischemic insult in neonatal brain.

Discussion

The present study demonstrates the specific involvement of NP1 within the cascade of biochemical events in mitochondria-mediated neuronal death, suggesting a novel mechanism of neuroprotection through modulation of NP1 expression against hypoxic-ischemic injury in neonatal brain. Firstly, the HI-induced NP1 interacts with the pro-death active Bax (NP1-Bax6A7) and translocate to mitochondria and this NP1-Bax6A7 association, in turn, promotes neuronal death through interaction with mtHKII and its detachment from mitochondria following HI. Furthermore, knockdown of NP1

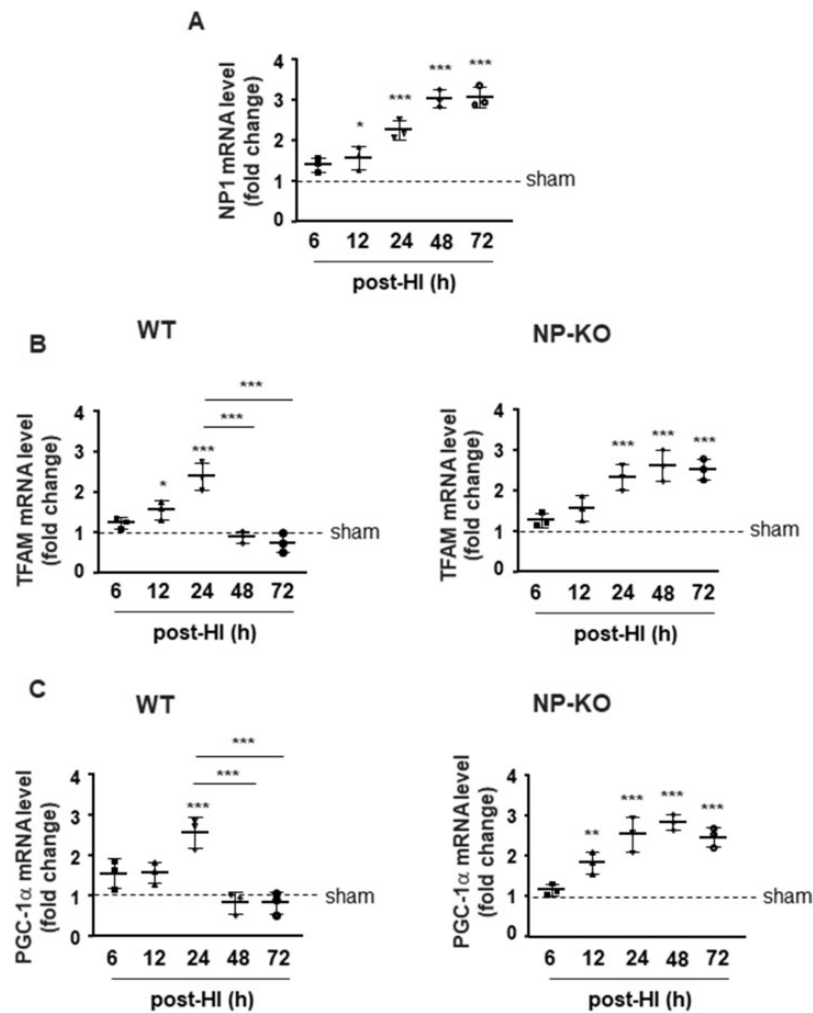


Figure 6. NP1 Gene Deletion Upholds Augmented Transcript Levels of Mitochondrial Biogenesis Factors in Response to HI. (A) NP1, (B) TFAM and (C) PGC-1 α mRNA expression was determined by RT-qPCR at indicated times and normalized to HPRT as described in materials and methods. A: NP1 mRNA levels in the cerebral cortex remained elevated following 6-72 h of HI, examined. Whereas, mRNA levels of mitochondrial biogenesis factors TFAM (B) and PGC-1 α (C) in the ipsilateral cortex of WT showed an early increase in both TFAM and PGC-1 α mRNA expression till 24 h, which significantly fell below at 48 h of post-HI and beyond. On the other hand, knocked down of NP1 gene maintained significantly increased mRNA expression levels of both *Tfam* (B) and PGC-1 α (C). Values are presented as mean \pm SD. (n = 3; *p < 0.05, **p < 0.01 and ***p < 0.001, one-way ANOVA followed by Bonferroni/Dunn post hoc test).

gene or inhibition of NP1 expression by GSK-3 inhibitor SB216763 blocked mtHKII dissociation from mitochondria under the conditions we observed NP1 inhibition and neuroprotection (Al Rahim et al., 2013). These findings provide a new molecular insight into the mechanisms linking NP1 in controlling mitochondria-mediated neuronal death and survival programs triggered by HI. Secondly, in demonstrating this we also show that mitochondrial accumulation of NP1 for prolonged periods after HI impairs mitochondrial biogenesis as evident by decreased expression of mitochondrial biogenesis-specific transcription factors TFAM and PGC-1 α . Strikingly, NP1 gene deletion augmented the expressions of TFAM and PGC-1 α as a measure to counteract the detrimental effects of HI on the neonatal brain, further

providing evidence for a new intracellular function of NP1. Taken together, our findings place NP1 within the paradigms of mitochondrial cell death and biogenesis program, and point to a novel target molecule to control both mitochondria-mediated neuronal death and mitochondrial repair mechanisms leading to neuroprotection in neonatal brain (Figure 8).

Mitochondrial dysfunction occurs as a consequence of HI, which place the brain at risk for compromised energy production and thus secondary injury (Yin et al., 2008). Conversely, endogenous protective pathways in mitochondria counteract the detrimental effects of HI through increased expressions of mitochondrial proteins and transcription factors involved in mitochondrial biogenesis (Yin et al., 2008; Valerio et al., 2011).

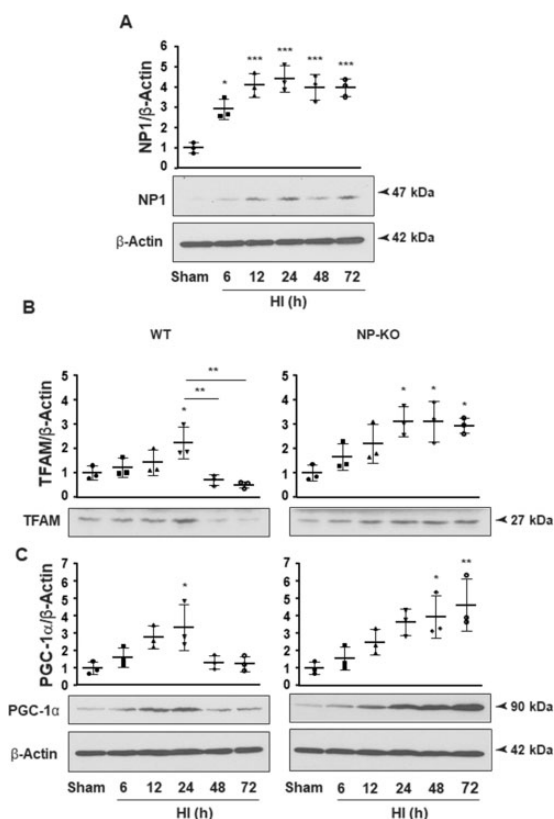


Figure 7. Knockdown of NPI Gene Expression Maintains Elevated Protein Expression of Mitochondrial Biogenesis Factors Following HI. A: NP1 protein levels remained up-regulated in the cerebral cortex following 6-72 h of HI. B and C: Expression of mitochondrial biogenesis factors TFAM and PGC-1 α in the cortex of WT and NP-KO mice. WB analyses showed an initial increase in TFAM (B) and PGC-1 α (C) protein levels, which were reduced substantially reduced at 48 h of post-HI and beyond. Interestingly, genetic deletion of NPI caused an unabated increase in the protein expression of the biogenesis factors TFAM and PGC-1 α , similar to that observed in case of mRNA expression compared to sham controls. Values are presented as mean \pm SD. (n = 3; *p < 0.05, **p < 0.01 and ***p < 0.001, one-way ANOVA followed by Bonferroni/Dunn post hoc test).

The contribution of NP1 in HI brain injury has been established by our laboratory (Hossain et al., 2004; Russell et al., 2011) and more recently, we have shown the involvement of NP1 in mitochondria-mediated neuronal death (Al Rahim et al., 2013). However, little is known about the effects of NP1 on pro-survival regulatory factors in mitochondria and transcriptional regulators of mitochondrial biogenesis under pathological stress. We found NP1 induction in the cerebral cortex occurred as early as 6 h post-HI, suggesting that the induction of NP1 is an early event triggering neuronal injury. On the other hand, the initial increase in the mtDNA content after HI (Yin et al., 2008) considered as an endogenous strategy to minimize cell damage, is attributable to lost energy due to the hypoxic-ischemic

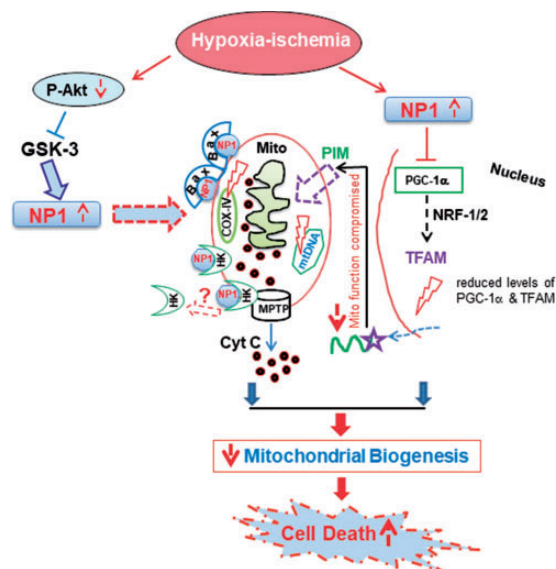


Figure 8. A Schematic Model Showing NPI Role in Mitochondrial Cell Death Mechanism and Biogenic Pathway. Ischemia induces NP1 expression and subsequent mitochondrial accumulation. Mitochondrial NP1 forms complexes with active Bax facilitating its mitochondrial localization, and interacts with HKII leading to its displacement from mitochondria. This dual effect pushes the cells towards the death pathway. Prolonged induction of NP1 following ischemia also causes impairment of mitochondrial compensatory mechanism by drastically downregulating the expressions of mitochondrial biogenesis factors, including TFAM and PGC-1, which are imported into mitochondrial subcompartments *via* the protein import machinery (PIM).

insult. In the present study, we found increased expression of the COX-1, which is exclusively mtDNA-encoded protein, but not the SDH-A (an nDNA-encoded protein), in response to HI. Comparable to the increase in mtDNA content and mtDNA-encoded COX-I, we also observed the up-regulation of mitochondrial-specific COXIV and HSP60 proteins following HI; responses reported to occur after many stressors (Kaufman et al., 2003; Sharma et al., 2014). Our data suggest that proteins encoded in the mitochondrion are perhaps more responsive to HI insult than those encoded in the nucleus, which lends credence to previous reports by others showing enhanced brain mtDNA content following HI injury. Furthermore, the mitochondrial accumulation of NP1 observed in our study is consistent with a previous report of increased amount of NP1 in mitochondria following low neuronal activity (Clayton et al., 2012). Our findings provided evidence that HI-induced NP1 was preferentially distributed in mitochondria-enriched fraction and its colocalization with MtDsRed further confirmed increased mitochondrial localization NP1 following OGD. Previously, we reported that NP1 facilitates mitochondrial translocation of pro-death protein Bax (Al Rahim et al., 2013). Here, we show that NP1's

association with active Bax, as evidenced by co-immunoprecipitation of NP1 with Bax6A7, leading to the activation of mitochondria-driven cell death program. On the other hand, the mtHKII acts as a powerful anti-apoptotic gatekeeper to suppress cell death, whereas detachment of mtHKII triggers apoptosis (Pastorino et al., 2002; Pastorino and Hoek, 2003; Vyssokikh and Brdiczka, 2004; Chiara et al., 2008). We observed HKII was abundantly present in mitochondria of normoxia cortical neurons, whereas, *in vitro* ischemia resulted in displacement of mtHKII and depletion of ATP levels with concurrent increase of NP1 protein accumulation in mitochondria. It appears that NP1 forms complex with active Bax (NP1-Bax6A7) in mitochondria and this complex, in turn, displaces HKII from VDAC site leading to mitochondrial membrane injury (Pastorino et al., 2002; Vyssokikh and Brdiczka, 2004). In addition, HKII displacement from mitochondrial has been shown following activation of GSK-3 β and Bax in renal ischemia (Pastorino and Hoek, 2003) whereas, inhibition of GSK-3 β blocked mtHKII dissociation and suppressed apoptosis (Gimenez-Cassina et al., 2009). On the other hand, overexpression of HKII decreases apoptosis by antagonizing “Bax attack” of the outer mitochondrial membrane (Gall et al., 2011). However, HKII overexpression has also been reported to improve survival after stress without preventing GSK-3 β or Bax activation (Gall et al., 2011), thus, suggesting the possibility of an intermediate regulatory molecule in the mechanism of HKII-regulated Bax-dependent mitochondrial membrane injury. Previously, we found GSK-3 α/β -dependent NP1 induction in OGD-exposed cortical and hippocampal neurons and that inhibition of GSK-3 suppressed NP1 expression (Russell et al., 2011; Al Rahim et al., 2013). It is likely that inhibition of NP1 induction with GSK-3 inhibitor or NP1 gene deletion could prevent OGD-induced mitochondrial translocation of active Bax (Al Rahim et al., 2013) and HKII dissociation from mitochondrial membrane, resulting in neuroprotection. These results together suggest that NP1 could be a control switch downstream of GSK-3 and upstream of HKII and Bax, thereby regulating mitochondrial injury and neuronal death following HI.

Mitochondrial biogenesis has been described in the context of cerebral hypoxic pre-conditioning (Gutsaeva et al., 2008) and neonatal HI (Yin et al., 2008), and that impaired mitochondrial biogenesis contributes to reduced mitochondrial function in OGD-exposed cortical neurons (Valerio et al., 2011). It is known that the coordinated action of PGC-1 α , NRF-1 and TFAM activate the mitochondrial biogenesis program (Scarpulla, 2006). Here, we have observed increased mRNA and protein expressions of PGC-1 α and TFAM during the early stages of HI (6-24 h) in WT brains which are consistent with earlier report demonstrating increased

mitochondrial biogenesis following HI (Yin et al., 2008). However, there is paucity of information examining the effects on mitochondrial biogenesis at longer periods after HI. Our data suggest that TFAM/PGC1 α levels go up initially as a compensatory mechanism but they progressively go down as NP1 expression and its translocation to mitochondria increases, as observed in later stages of ischemia (48-72 h post-HI), which is in line with the profound reduction of mtDNA content reported after ischemic insult (Chen et al., 2001). Thus, restoration of TFAM/PGC1 α levels in HI model will increase mitochondrial biogenesis and stabilize neuronal function through increasing mitochondrial activity (Scarpulla, 2006; Valerio et al., 2011). Ablation of NP1 gene led to a persistent elevation of TFAM/PGC1 α levels, at least for 72 h post HI. This unabated augmentation of the mitochondrial biogenesis program in the NP1-KO brain perhaps account for the neuroprotection observed in the NP1-KO brain against HI (Thatipamula et al., 2015). Hence, it can be concluded that compensatory mechanisms that are neuroprotective during HI injury involve the presence of TFAM/PGC1 α which otherwise are depleted in brain tissue death. In agreement with our *in vivo* studies, our preliminary findings suggest mitochondrial anterograde movement in OGD-exposed cortical neurons (data not shown), which is the subject of our future studies. The transport of mitochondria to the area of high energy demand is essential for neuronal viability (Rintoul and Reynolds, 2010). The PGC-1 α has roles in both mitochondrial biogenesis and transport (Scarpulla, 2006; O'Donnell et al., 2013), and that NP1 gene deletion enhanced PGC-1 α expression following HI; suggesting a possible role of NP1 in mitochondrial anterograde transport *via* regulating PGC-1 α expression.

In conclusion, our findings place NP1 as a key molecule controlling neuronal susceptibility to mitochondria-mediated neuronal death or survival in response to hypoxic-ischemic insult in neonatal brain. The enhanced expression of NP1 following HI occurs upstream of both Bax and HKII and that NP1 interacts with active Bax. It is possible that this NP1-Bax6A7 association could subsequently leads to HKII displacement from mitochondria and neuronal death. Most importantly, our findings also demonstrate the involvement of NP1 in impaired mitochondrial biogenesis in HI-induced delayed neuronal death possibly through down regulation of PGC-1 α and TFAM. In contrast, the genetic deletion of NP1 augmented the expressions of the biogenesis factors in response to prolonged HI. Our findings provide important insights into the function of NP1 within the mitochondria-specific biochemical events initiated at diverse points of hypoxic-ischemic insult. Our results point to a novel molecular target in preventing hypoxic-ischemic brain injury in neonates *via*

improvement of mitochondrial biogenesis and reduced mitochondrial injury.

Declaration of Conflicting Interests

The author(s) declared no potential conflicts of interest with respect to the research, authorship, and/or publication of this article.

Funding

The author(s) disclosed receipt of the following financial support for the research, authorship, and/or publication of this article: This work was supported by the National Institutes of Health grant RO1NS046030-09, P50 AT008661-01 and by the Alzheimer's Association grant AARF-17-531426.

ORCID iD

Md Al Rahim  <https://orcid.org/0000-0002-8556-0351>

References

- Achanta, G., Sasaki, R., Feng, L., Carew, J. S., Lu, W., Pelicano, H., Keating, M. J., & Huang, P. (2005). Novel role of p53 in maintaining mitochondrial genetic stability through interaction with DNA pol gamma. *The Embo Journal*, *24*(19), 3482–3492.
- Al Rahim, M., & Hossain, M. A. (2013). Genetic deletion of NP1 prevents hypoxic-ischemic neuronal death via reducing AMPA receptor synaptic localization in hippocampal neurons. *Journal of the American Heart Association*, *2*(1), e006098.
- Al Rahim, M., Nakajima, A., Saigusa, D., Tetsu, N., Maruyama, Y., Shibuya, M., Yamakoshi, H., Tomioka, Y., Iwabuchi, Y., Ohizumi, Y., & Yamakuni, T. (2009). 4'-Demethylnobiletin, a bioactive metabolite of nobiletin enhancing PKA/ERK/CREB signaling, rescues learning impairment associated with NMDA receptor antagonism via stimulation of the ERK Cascade. *Biochemistry*, *48*(32), 7713–7721.
- Al Rahim, M., Thatipamula, S., & Hossain, M. A. (2013). Critical role of neuronal pentraxin 1 in mitochondria-mediated hypoxic-ischemic neuronal injury. *Neurobiology of Disease*, *50*, 59–68.
- Barks, J. D., & Silverstein, F. S. (1992). Excitatory amino acids contribute to the pathogenesis of perinatal hypoxic-ischemic brain injury. *Brain Pathology (Zurich, Switzerland)*, *2*(3), 235–243.
- Blomgren, K., & Hagberg, H. (2006). Free radicals, mitochondria, and hypoxia-ischemia in the developing brain. *Free Radical Biology & Medicine*, *40*(3), 388–397.
- Chen, H., Hu, C. J., He, Y. Y., Yang, D. I., Xu, J., & Hsu, C. Y. (2001). Reduction and restoration of mitochondrial DNA content after focal cerebral ischemia/reperfusion. *Stroke*, *32*(10), 2382–2387.
- Cheng, Y., Deshmukh, M., D'Costa, A., Demaro, J. A., Gidday, J. M., Shah, A., Sun, Y., Jacquin, M. F., Johnson, E. M., & Holtzman, D. M. (1998). Caspase inhibitor affords neuroprotection with delayed administration in a rat model of neonatal hypoxic-ischemic brain injury. *The Journal of Clinical Investigation*, *101*(9), 1992–1999.
- Chiara, F., Castellaro, D., Marin, O., Petronilli, V., Brusilow, W. S., Juhaszova, M., Sollott, S. J., Forte, M., Bernardi, P., & Rasola, A. (2008). Hexokinase II detachment from mitochondria triggers apoptosis through the permeability transition pore independent of voltage-dependent anion channels. *PLoS One*, *3*(3), e1852.
- Clayton, K. B., Podlesniy, P., Figueiro-Silva, J., López-Doménech, G., Benitez, L., Enguita, M., Abad, M. A., Soriano, E., & Trullas, R. (2012). NP1 regulates neuronal activity-dependent accumulation of BAX in mitochondria and mitochondrial dynamics. *The Journal of Neuroscience: The Official Journal of the Society for Neuroscience*, *32*(4), 1453–1466.
- Colombini, M. (2004). VDAC: The channel at the interface between mitochondria and the cytosol. *Molecular and Cellular Biochemistry*, *256*(1/2), 107–115.
- Fiskum, G. (2000). Mitochondrial participation in ischemic and traumatic neural cell death. *Journal of Neurotrauma*, *17*(10), 843–855.
- Gall, J. M., Wong, V., Pimental, D. R., Havasi, A., Wang, Z., Pastorino, J. G., Bonegio, R. G. B., Schwartz, J. H., & Borkan, S. C. (2011). Hexokinase regulates bax-mediated mitochondrial membrane injury following ischemic stress. *Kidney International*, *79*(11), 1207–1216.
- Galluzzi, L., Blomgren, K., & Kroemer, G. (2009). Mitochondrial membrane permeabilization in neuronal injury. *Nature Reviews. Neuroscience*, *10*(7), 481–494.
- Gimenez-Cassina, A., Lim, F., Cerrato, T., Palomo, G. M., & Diaz-Nido, J. (2009). Mitochondrial hexokinase II promotes neuronal survival and acts downstream of glycogen synthase kinase-3. *The Journal of Biological Chemistry*, *284*(5), 3001–3011.
- Gupta, S., & Knowlton, A. A. (2002). Cytosolic heat shock protein 60, hypoxia, and apoptosis. *Circulation*, *106*(21), 2727–2733.
- Gutsaeva, D. R., Carraway, M. S., Suliman, H. B., Demchenko, I. T., Shitara, H., Yonekawa, H., & Piantadosi, C. A. (2008). Transient hypoxia stimulates mitochondrial biogenesis in brain subcortex by a neuronal nitric oxide synthase-dependent mechanism. *The Journal of Neuroscience: The Official Journal of the Society for Neuroscience*, *28*(9), 2015–2024.
- Hagberg, H. (2004). Mitochondrial impairment in the developing brain after hypoxia-ischemia. *Journal of Bioenergetics and Biomembranes*, *36*(4), 369–373.
- Halestrap, A. P., Doran, E., Gillespie, J. P., & O'Toole, A. (2000). Mitochondria and cell death. *Biochemical Society Transactions*, *28*(2), 170–177.
- Hossain, M. A., Fielding, K. E., Trescher, W. H., Ho, T., Wilson, M. A., & Lattera, J. (1998). Human FGF-1 gene delivery protects against quinolinate-induced striatal and hippocampal injury in neonatal rats. *European Journal of Neuroscience*, *10*(8), 2490–2499.
- Hossain, M. A., Russell, J. C., & O'Brien, R. (2004). Neuronal pentraxin 1: A novel mediator of hypoxic-ischemic injury in neonatal brain. *Journal of Neuroscience*, *24*(17), 4187–4196.
- Hsu, Y. T., & Youle, R. J. (1998). Bax in murine thymus is a soluble monomeric protein that displays differential

- detergent-induced conformations. *The Journal of Biological Chemistry*, 273(17), 10777–10783.
- Kaufman, B. A., Kolesar, J. E., Perlman, P. S., & Butow, R. A. (2003). A function for the mitochondrial chaperonin Hsp60 in the structure and transmission of mitochondrial DNA nucleoids in *Saccharomyces cerevisiae*. *The Journal of Cell Biology*, 163(3), 457–461.
- Majewski, N., Nogueira, V., Bhaskar, P., Coy, P. E., Skeen, J. E., Gottlob, K., Chandel, N. S., Thompson, C. B., Robey, R. B., & Hay, N. (2004). Hexokinase-mitochondria interaction mediated by akt is required to inhibit apoptosis in the presence or absence of bax and bak. *Molecular Cell*, 16(5), 819–830.
- Mattson, M. P., Gleichmann, M., & Cheng, A. (2008). Mitochondria in neuroplasticity and neurological disorders. *Neuron*, 60(5), 748–766.
- O'Donnell, K. C., Vargas, M. E., & Sagasti, A. (2013). WldS and PGC-1 α regulate mitochondrial transport and oxidation state after axonal injury. *The Journal of Neuroscience: The Official Journal of the Society for Neuroscience*, 33(37), 14778–14790.
- Pastorino, J. G., & Hoek, J. B. (2003). Hexokinase II: The integration of energy metabolism and control of apoptosis. *Current Medicinal Chemistry*, 10(16), 1535–1551.
- Pastorino, J. G., Hoek, J. B., & Shulga, N. (2005). Activation of glycogen synthase kinase 3 β disrupts the binding of hexokinase II to mitochondria by phosphorylating voltage-dependent anion channel and potentiates chemotherapy-induced cytotoxicity. *Cancer Research*, 65(22), 10545–10554.
- Pastorino, J. G., Shulga, N., and., & Hoek, J. B. (2002). Mitochondrial binding of hexokinase II inhibits bax-induced cytochrome c release and apoptosis. *The Journal of Biological Chemistry*, 277(9), 7610–7618.
- Rintoul, G. L., & Reynolds, I. J. (2010). Mitochondrial trafficking and morphology in neuronal injury. *Biochimica et Biophysica Acta*, 1802(1), 143–150.
- Russell, J. C., Kishimoto, K., O'Driscoll, C., & Hossain, M. A. (2011). Neuronal pentraxin 1 induction in hypoxic-ischemic neuronal death is regulated via a glycogen synthase kinase-3 α /3 β dependent mechanism. *Cellular Signalling*, 23(4), 673–682.
- Scarpulla, R. C. (2006). Nuclear control of respiratory gene expression in mammalian cells. *Journal of Cellular Biochemistry*, 97(4), 673–683.
- Sharma, J., Johnston, M. V., and., & Hossain, M. A. (2014). Sex differences in mitochondrial biogenesis determine neuronal death and survival in response to oxygen glucose deprivation and reoxygenation. *BMC Neuroscience*, 15(1), 9.
- St-Pierre, J., Drori, S., Uldry, M., Silvaggi, J. M., Rhee, J., Jäger, S., Handschin, C., Zheng, K., Lin, J., Yang, W., Simon, D. K., Bachoo, R., & Spiegelman, B. M. (2006). Suppression of reactive oxygen species and neurodegeneration by the PGC-1 transcriptional coactivators. *Cell*, 127(2), 397–408.
- Thatipamula, S., Al Rahim, M., Zhang, J., & Hossain, M. A. (2015). Genetic deletion of neuronal pentraxin 1 expression prevents brain injury in a neonatal mouse model of cerebral hypoxia-ischemia. *Neurobiology of Disease*, 75, 15–30.
- Valerio, A., Bertolotti, P., Delbarba, A., Perego, C., Dossena, M., Ragni, M., Spano, P., Carruba, M. O., De Simoni, M. G., & Nisoli, E. (2011). Glycogen synthase kinase-3 inhibition reduces ischemic cerebral damage, restores impaired mitochondrial biogenesis and prevents ROS production. *Journal of Neurochemistry*, 116(6), 1148–1159.
- Vyssokikh, M., & Brdiczka, D. (2004). VDAC and peripheral channelling complexes in health and disease. *Molecular and Cellular Biochemistry*, 256–257(1–2), 117–126.
- Wu, C., Zhan, R. Z., Qi, S., Fujihara, H., Taga, K., & Shimoji, K. (2001). A forebrain ischemic preconditioning model established in C57Black/Crj6 mice. *Journal of Neuroscience Methods*, 107(1–2), 101–106.
- Yin, W., Signore, A. P., Iwai, M., Cao, G., Gao, Y., & Chen, J. (2008). Rapidly increased neuronal mitochondrial biogenesis after hypoxic-ischemic brain injury. *Stroke*, 39(11), 3057–3063.
- Youle, R. J., & Strasser, A. (2008). The BCL-2 protein family: Opposing activities that mediate cell death. *Nature Reviews Molecular Cell Biology*, 9(1), 47–59.
- Zaid, H., Abu-Hamad, S., Israelson, A., Nathan, I., & Shoshan-Barmatz, V. (2005). The voltage-dependent anion channel-1 modulates apoptotic cell death. *Cell Death and Differentiation*, 12(7), 751–760.